Journal of Structural Engineering. Submitted November 8, 2011; accepted July 20, 2012;
posted ahead of print August 11, 2012. doi:10.1061/(ASCE)ST.1943-541X.0000677

Truss-Arch Model for Shear Strength of Shear-Critical Reinforced Concrete Columns

Zuanfeng Pan[1] and Bing Li[2]

Abstract:

Experimental observations on 11 Reinforced Concrete (RC) columns tested at Nanyang Technological University (NTU), and existing experimental data of 79 shear-critical RC columns are presented. Significant arch action is found in columns of small shear span-to-depth ratio and high axial-load ratio under shear force. Utilizing the sectional method for shear strength of these types of columns, which does not consider arch action, would give a more conservative prediction. Based on the truss-arch model, an expression to predict the shear strength of shear-critical RC columns is presented, which considers both the contributions of concrete and transverse reinforcement to shear strength in the truss model as well as the contribution of arch action through compatibility of deformation. The proposed model is compared with other shear strength models using the available column test data consisting of 90 shear-critical RC columns, and the results show that the proposed model can improve the accuracy of shear strength predictions for shear-critical RC columns.

CE Database subject headings: Shear strength; Reinforced concrete columns; Experimental observation; Truss-arch model; Truss model; Arch action; Shear span-to-depth ratio; Axial-load ratio.

---

[1]Lecturer, School of Civil Engineering at Southeast University, China, 210096.

[2]Associate Professor, School of Civil and Environmental Engineering at Nanyang Technological University, Singapore, 639798.

Journal of Structural Engineering. Submitted November 8, 2011; accepted July 20, 2012;
posted ahead of print August 11, 2012. doi:10.1061/(ASCE)ST.1943-541X.0000677

Introduction

A large number of existing RC columns in zones of low to moderate seismicity have not been designed as per the requirements of modern seismic design codes. These are generally termed as non-seismically detailed RC columns. Vital deficiencies in such columns include typical reinforcement details like widely spaced and poorly anchored transverse reinforcements. Recent post-earthquake investigations have indicated that these non-seismically detailed RC columns are vulnerable to shear failure, which would drastically reduce their seismic performance and usually lead to structural collapse during earthquakes, as shown in Fig. 1. The brittle failure modes, such as shear failure, must be inhibited to satisfy the requirement of seismic response of reinforced concrete structures. Hence, for existing concrete structures, a thorough evaluation of non-seismically detailed RC columns is needed to mitigate shear failure under earthquake loading, while for new concrete structures, the RC columns must be designed with sufficient shear capacity to sustain the whole building in the event of an earthquake. The objective of this paper is to develop a sound model that is capable of predicting the shear strength of shear-critical RC columns.

Over the last century, many researchers have developed sectional models or semi-empirical theories based on extensive experimental data to predict the shear strength of RC columns. However, the use of sectional models such as the variable angle truss model or the modified compression field theory (ASCE-ACI Committee 445 1998) to predict the shear strength fails to consider the arch action in the column, and is therefore more conservative. Arch action in RC members subjected to shear force has been recognized by many researchers (Leonhardt 1965; Ichinose 1992; Kim *et al*. 1998). Leonhardt (1965) proposed a truss model with inclined compression chords to describe the behavior of arch action in RC beams; in his model, parts of the shear is carried by the inclined compression

Journal of Structural Engineering. Submitted November 8, 2011; accepted July 20, 2012;
posted ahead of print August 11, 2012. doi:10.1061/(ASCE)ST.1943-541X.0000677

chord; the rest of the shear is sustained by the web through the truss model. Kim *et al.* (1998) developed this type of truss-arch model in RC beams, and predicted the arch profile and quantified the intensity of arch action by means of the smeared truss idealization technique as well as experimental investigations on RC beams. Based on the experimentally measured steel tensions over the shear span in the RC beams, Kim *et al*. (1998) proposed an empirical coefficient, α, which represents arch action contribution to total shear capacity. Ichinose (1992) presented a truss-arch model as shown in Fig. 2, and proposed a design equation to prevent shear failure after flexural inelastic deformation, which has been adopted in the AIJ Design Guidelines (1994). However, in the derivation of the shear design equation (Ichinose 1992) for RC columns, the condition of deformation compatibility between the truss and the arch has not been accounted for, and the height of the strut arch is assumed to be half the height of the column, which does not match the experimental observation. Moreover, in the truss model, the contribution of concrete to shear, such as the aggregate interlock on the crack surface, has not been considered.

This paper presents experimental observations on 90 shear-critical RC columns of which observations on 11 columns were from tests conducted at NTU and another 79 columns collected from the literature. In this study, a truss-arch model to predict the shear strength of shear-critical RC columns is developed based on Ichinose's shear strength model (1992). This model can reasonably represent the contributions of shear span-to-depth ratio, a/d and the axial-load ratio, $P/(f_c'A_g)$ to the shear strength of RC columns. As an improvement to Ichinose's shear model, deformation compatibility between the truss model and the arch model as well as a more reasonable effective depth for the arch model are considered in this model. The validity of the proposed model has been verified by the test data of 90 shear-critical RC columns, and is compared with other shear models.

Journal of Structural Engineering. Submitted November 8, 2011; accepted July 20, 2012;
posted ahead of print August 11, 2012. doi:10.1061/(ASCE)ST.1943-541X.0000677

Observed Experimental Results

Arch action is significant in RC columns which have been subjected to the combined action of shear, flexure and axial compressive force. It is well known that the shear strength of RC column increases as the shear span-to-depth ratio decreases. As members become deeper or shorter, more shear force will be transmitted directly to the support by a compressive strut rather than flexure. Another important factor influencing arch action is the axial load on the section (due to an applied load or prestressing). The influences of axial load on shear are threefold. Firstly, the compressive force can increase the neutral axis depth of the section; secondly, the angle of the inclined crack can be decreased due to the compressive force; thirdly, the crack width can be reduced and the ability of the crack interface to transmit the shear increases. The first influence can be represented by arch action, whereas the other two influences can be illustrated by the truss model.

Experimental Observation at NTU

A total of 11 columns were studied experimentally to examine the shear strength of RC columns with light transverse reinforcement. The experiments were conducted by Tran and Li (2010) at the Protective Engineering Laboratory at NTU, Singapore. These specimens were tested under a combination of cyclic shear force and constant axial load to simulate earthquake action. The main parameters in the experiment included shear span-to-depth ratio, a/d and axial-load ratio, $P/(f_c'A_g)$. Fig. 3 and Table 1 provide the experimental parameters and details of the columns. Reversed horizontal displacements were applied to the specimen using an actuator with a 1000kN capacity whose axis passed through the mid-height of the specimen, thus generating a double-bending loading condition to the specimen. The column axial load was applied slowly to the specimens until the targeted level of displacement was achieved. During each test, the column axial load was

Journal of Structural Engineering. Submitted November 8, 2011; accepted July 20, 2012;
posted ahead of print August 11, 2012. doi:10.1061/(ASCE)ST.1943-541X.0000677

maintained by manually adjusting the vertical actuators after each load step.

The longitudinal steels consisted of two bar types: eight 20mm diameter deformed bars with a yield stress f_y = 408MPa; and eight Dia. 25 mm deformed bars with a yield stress of 409MPa, as shown in Table 1. The 6 mm diameter mild-steel bars with a yield stress f_{vy} = 392.6MPa were used for the stirrups. The average cylinder compressive strengths measured on the days of testing for each specimen are summarized in Table 1. More details of the specimens can be found in Tran (2010).

Figs. 4, 5 and 6 show the comparison of the backbone curves of the SC-2.4, SC-1.7 and RC-1.7 series of specimens respectively. Comparisons are made based on the general profile of the backbone curves, shear strength, and the drift ratios at shear failure and axial failure. Shear failure of the tested column is defined as the recorded shear force when the shear-resisting capacity drops by more than 20% of the maximum shear force, while axial failure occurs once the column is no longer able to resist the applied axial force. Due to the light transverse reinforcement, typical brittle shear failure backbone curves are observed in all specimens. Figs. 4, 5 and 6 indicate that the drift ratios at shear failure in all specimens are less than 2.0%, except for Specimen RC-1.7-0.05.

From Fig. 4, the shear strength is increased by around 8.5% as the axial-load ratio is increased from 0.20 to 0.50. The compressive strength of Specimen SC-2.4-0.30 is greater than the other two specimens in the same series; therefore its shear strength is excluded from comparison with the other two. As seen in Fig. 5, the shear strength of the SC-1.7 series of specimens was enhanced by about 6.4%, 21.4%, and 35.9% as the axial load ratio was increased from 0.05 to 0.20, 0.35 and 0.50, respectively. From Fig. 6, the shear strength of RC-1.7 series of specimens was enhanced by about 7.9%, 22.1%, and 25.5% as the axial load ratio was increased from 0.05 to 0.20, 0.35 and 0.50, respectively. The aforementioned discussion clearly indicates that the axial compressive force

Journal of Structural Engineering. Submitted November 8, 2011; accepted July 20, 2012;
posted ahead of print August 11, 2012. doi:10.1061/(ASCE)ST.1943-541X.0000677

can enhance the arch action of the column under shear. In addition, the influence of shear span-to-depth ratio on shear strength can be observed for Specimens SC-2.4-0.20 and SC-1.7-0.20, and for Specimens SC-2.4-0.50 and SC-1.7-0.50. An increase in shear strength for Specimens SC-2.4-0.20 and SC-1.7-0.20 was 34.4%, and an enhancement of 58.1% in shear strength was observed for Specimens SC-2.4-0.50 and SC-1.7-0.50. From the shear strength enhancement, it can be concluded that arch action becomes increasingly marked with a decrease in shear span-to-depth ratio or an increase in axial-load ratio in RC columns.

Experimental Database of Shear-Critical RC Columns

A database consisting of 79 shear-critical RC columns has been considered in this study, and the details of these RC columns are shown in Appendix. Fig. 7 shows that normalized shear strength decreases with increasing shear span-to-depth ratio within the range of test data considered. Fig. 8 shows the relationship between the normalized shear strength and the axial-load ratio. The data trend suggests shear strength increases with an increasing axial-load ratio.

Therefore, for RC columns with small shear span-to-depth ratio or high axial-load ratio, the Bernoulli's hypothesis of plain strain distribution is invalid, and parts of the shear force are directly transmitted by arch action via the compressive strut. This points to an over-conservative estimate of shear strength by the sectional model, especially for RC columns of small shear span-to-depth ratio or high axial-load ratio. Therefore, it is possible to develop a more reasonable truss-arch model to represent the shear strength for RC columns.

Truss-Arch Model for Shear Strength

From the observation on previously tested RC columns, the distribution of the inclined cracks is seen as such: the inclined crack angle with respect to the longitudinal axis of column, θ, decreases

Journal of Structural Engineering. Submitted November 8, 2011; accepted July 20, 2012;
posted ahead of print August 11, 2012. doi:10.1061/(ASCE)ST.1943-541X.0000677

as the distance to the restrained end increases, after reaching the minimum angles, and then the diagonal cracks look almost parallel. This phenomenon of diagonal cracks pattern is also verified by the specimens shown in Table 1. Fig. 9 shows the cracks patterns of Specimens SC-2.4-0.20 and SC-2.4-0.30 at shear failure and at axial failure. As mentioned above, the shear failure of tested columns is defined as the recorded shear force when the shear-resisting capacity drops by more than 20% of the maximum shear force. The shear behavior of RC columns can be described by means of the variable angle truss model with a compressive strut arch in terms of the diagonal cracks pattern shown in Fig. 10(*a*). However, the variable angle truss model with a compressive strut arch is statically indeterminate, and is of limited applicability in practice. The behavior of the variable angle truss can be approximately represented by the constant angle truss model with shear span $a > d_v\cot\theta$ (Kim and Mander 1999). Here, based on the truss model with a compressive strut arch, an expression has been developed to analytically predict the shear strength of RC columns, considering the compatibility of deformation between the truss model and the arch model. The components of shear strength for a shear-critical RC column are illustrated in Fig. 10(*b*). The shear strength of the column consisting of three parts is as follows,

$$V_n = V_{ct} + V_s + V_a \tag{1}$$

in which V_{ct}, V_s are the contributions of concrete and transverse reinforcements to the shear in the truss model respectively; and V_a is the shear strength provided by the arch action.

Truss Component

The contribution of concrete and transverse reinforcement to shear in the truss model is based on the Modified Compression Field Theory (MCFT) (Vecchio and Collins 1986). The contribution of transverse reinforcement to shear can be expressed as:

Journal of Structural Engineering. Submitted November 8, 2011; accepted July 20, 2012;
posted ahead of print August 11, 2012. doi:10.1061/(ASCE)ST.1943-541X.0000677

$$V_s = \frac{A_{sv} f_{vy} d_v \cot\theta}{s} \tag{2}$$

From Fig. 10(*b*), the concrete contribution to shear strength in the truss model, V_{ct} is assumed as the amount of force transferred across the crack interface. V_{ct} (Benz *et al.* 2006) is expressed as:

$$V_{ct} = \beta b d_v \sqrt{f_c'} \tag{3}$$

Bentz *et al.* (2006) gave a simplified method to calculate the value of β:

$$\beta = \frac{0.40}{1+1500\varepsilon_x} \times \frac{1300}{1000+s_{ze}} \tag{4}$$

in which ε_x is the longitudinal strain at the mid-depth of cross-section, and can be computed by Eq. (5); s_{ze} is the effective crack spacing, and for members with stirrups, the stirrups will control the crack spacing and the term s_{ze} can be simply taken as 300mm (CSA 2004).

$$\varepsilon_x = \frac{\frac{V_t L}{\zeta_1 d_v} - 0.5P + 0.5V_t \cot\theta}{2E_s A_s} \tag{5}$$

where ζ_1 is the factor of boundary condition for calculating ε_x, ζ_1 =2 for fixed-fixed ends, ζ_1 =1 for fixed-pinned ends; V_t is the lump-summed V_{ct} and V_s in the truss model, $V_t = V_{ct} + V_s$.

Few reliable methods exist for estimating the angle θ. Priestley *et al.* (1994) suggested that the angle of shear plane of a RC column could be taken as 60 degrees. For the columns tested by Lynn (2001) and Sezen (2002), the critical angle, Elwood *et al.* (2005) proposed $\theta = 55+35P/P_0$, and P_0 is the axial capacity of the undamaged column given by $0.85f_c'(A_g - A_s)+f_y A_s$, in which A_{sl} is the area of longitudinal steel. However, this formula is found based on the columns tested by Lynn (2001) and Sezen (2002). A model proposed by Kim and Mander (1999, 2007) estimates the crack angle based on minimizing the external work due to a unit shear force, which is more reasonable and calibrated by experimental observations. The expression for θ (Kim and Mander 1999) is as follows,

Journal of Structural Engineering. Submitted November 8, 2011; accepted July 20, 2012;
posted ahead of print August 11, 2012. doi:10.1061/(ASCE)ST.1943-541X.0000677

$$\theta = \arctan\left(\frac{n\rho_v + \zeta_2 \dfrac{\rho_v b d_v}{\rho_{sl} A_g}}{1 + n\rho_v}\right)^{1/4} \tag{6}$$

where ζ_2 is the factor of boundary condition of the column for calculating θ, ζ_2=0.57 for fixed-fixed ends, and ζ_2=1.57 for fixed-pinned ends.

In Eq. (5), 0.5cotθ is approximately equal to 1.0, which is also accepted in CSA-04 (2004). By substituting $V_t = V_{ct} + V_s$ into Eq. (5), combined with Eqs. (2) through (4), we will get:

$$\frac{\dfrac{520\sqrt{f_c'}bd_v}{V_{ct}\left(1000 + s_{ze}\right)} - 1}{1500} = \frac{\left(\dfrac{A_{sv}f_{vy}}{s} d_v \cot\theta + V_{ct}\right)L}{\zeta_1 d_v} - 0.5P + \frac{A_{sv}f_{vy}}{s} d_v \cot\theta + V_{ct}}{2E_s A_s} \tag{7}$$

Therefore, the concrete contribution to shear strength in the truss model is:

$$V_{ct} = \frac{-B + \sqrt{B^2 - 4AC}}{2A} \tag{8}$$

in which $A = \dfrac{750}{E_s A_s}\left(1 + \dfrac{L}{\varsigma_1 d_v}\right)$, $B = \dfrac{750V_s}{E_s A_s}\left(1 + \dfrac{L}{\varsigma_1 d_v}\right) - \dfrac{375P}{E_s A_s} + 1$, $C = \dfrac{-520\sqrt{f_c'}bd_v}{1000 + s_{ze}}$

Arch Component

Arch action is assumed to be related to a single compressive strut directed from the compression zone at the top towards that at the bottom, as shown in Fig. 11. If the RC column is in double bending, the inclination of the strut is found from the line joining the centers of flexural compression at the top and at the bottom of the column, as shown in Fig. 11(*a*). If the RC column is in single bending, the inclination of the strut is formed at the axis at the top and the center of flexural compression at the bottom of the column, as shown in Fig. 11(*b*). It will be apparent that there are similarities to the arch action of Ichinose's model (1992) and Priestley *et al*'s model (1994), although Ichinose's model is independent of the axial load level, while in Priestley *et al*'s

Journal of Structural Engineering. Submitted November 8, 2011; accepted July 20, 2012;
posted ahead of print August 11, 2012. doi:10.1061/(ASCE)ST.1943-541X.0000677

model, the arch contribution to shear, V_p is related with the axial load P, $V_p = P \tan\alpha$, and both of them do not consider the condition of deformation compatibility between the truss model and the arch model. Here, the arch contribution is derived from the condition of deformation compatibility between the truss model and the arch model. The shear deformation induced by the truss model must be equal to that induced by the arch model. That is:

$$\frac{V_t}{K_t} = \frac{V_a}{K_a} \tag{9}$$

in which K_a and K_t are the shear stiffness of the strut arch model and the truss model, respectively. The shear deformation of the truss is caused by the elongation of transverse ties and the compression of the inclined struts, as shown in Fig. 12. The length of the diagonal concrete strut is $d_v/\sin\theta$, the width of the diagonal concrete compression strut is $d_v\cos\theta$; under shear force V_t, the diagonal concrete compression strain is obtained.

$$\varepsilon_c = \frac{V_t}{E_c b d_v \sin\theta\cos\theta} \tag{10}$$

Therefore, the shortening of the diagonal strut is

$$\Delta_c = \varepsilon_c \frac{d_v}{\sin\theta} = \frac{V_t}{bE_c \sin^2\theta\cos\theta} \tag{11}$$

The lateral displacement induced by the compression of struts under V_t is as follows,

$$\delta_c = \frac{\Delta_c}{\sin\theta} = \frac{V_t}{E_c b \sin^3\theta\cos\theta} \tag{12}$$

The elongation of the transverse steels is

$$\delta_s = \frac{f_{vs}}{E_s} d_v = \frac{d_v V_t}{E_s A_{sv0}} = \frac{V_t}{E_s \rho_v b \cot\theta} \tag{13}$$

The responding shear rotation is then calculated by dividing the sum of Eq. (12) and Eq. (13) by the vertical length of a single crack ($d_v\cot\theta$), thus,

$$\gamma_t = \left(\delta_c + \delta_s\right) / \left(d_v \cot\theta\right) \tag{14}$$

Journal of Structural Engineering. Submitted November 8, 2011; accepted July 20, 2012;
posted ahead of print August 11, 2012. doi:10.1061/(ASCE)ST.1943-541X.0000677

Therefore, the shear stiffness of the truss model is:

$$K_t = \frac{V_t}{\gamma_t} = \frac{n\rho_v E_c b d_v \cot^2\theta}{1 + n\rho_v \csc^4\theta} \tag{15}$$

Eq. (15) is identical to the expression developed by Kim and Mander (1999).

For the arch model, the shear formation is induced by the compression of the strut, and as shown in Fig. 11(*a*). The width of the arch strut is $c_a\cos\alpha$, where c_a is the effective depth of strut in arch model. For the RC columns under cyclic loading, the concrete cover will partly flake off when the maximum shear force is reached, therefore c_a will decrease, here c_a can be taken as $c_a = x–c$. Under shear force, V_a, the diagonal concrete compression strain is obtained,

$$\varepsilon_a = \frac{V_a}{\sin\alpha E_c b c_a \cos\alpha} \tag{16}$$

The lateral displacement induced by the compression of struts under shear force, V_a is as follows,

$$\delta_a = \frac{\Delta_a}{\sin\alpha} = \frac{V_a L}{E_c b c_a \sin^2\alpha\cos^2\alpha} \tag{17}$$

We can get the shear stiffness of the arch model as follows,

$$K_a = \frac{V_a}{\gamma_a} = \frac{V_a}{\delta_a / L} = E_c b c_a \sin^2\alpha\cos^2\alpha \tag{18}$$

in which γ_a is the shear rotation; α is the inclination of the strut; for column in double bending as shown in Fig. 11(*a*), $\alpha = (h–x)/L$; for column in single bending, as shown in Fig. 11(*b*), $\alpha = (h–x)/(2L)$. The neutral axis depth, x can be estimated as follows (Paulay and Priestley's 1992):

$$x = \left(0.25 + 0.85\frac{P}{f_c' A_g}\right) h \tag{19}$$

So the shear strength of RC column under monotonic loading is:

$$V_m = V_{ct} + V_s + V_a = \left(V_{ct} + V_s\right)\left(1 + \frac{K_a}{K_t}\right) \tag{20}$$

Journal of Structural Engineering. Submitted November 8, 2011; accepted July 20, 2012;
posted ahead of print August 11, 2012. doi:10.1061/(ASCE)ST.1943-541X.0000677

Impact of Displacement Ductility on Shear Strength

It has long been proven that repeated loading results in a series of intersecting cracks, and the widening of existing cracks. The widening of shear cracks reduces the aggregate interlock effect of the crack interface, which would decrease the shear strength. Furthermore, the effective compressive strength of concrete decreases as more and more intersecting shear cracks appear in the column. Using the test data from ductile and unductile RC columns, Konwinski *et al.* (1996) concluded that shear strength was independent of displacement ductility. On the other hand, Priestley *et al.* (1994) and Sezen *et al.*(2002, 2004) believed that shear strength had a relation with the member displacement ductility level. The difference is, however, that Priestley *et al.* (1994) proposed the concrete contribution to shear was decreased as the member displacement ductility increased, while Sezen (2002) suggested that both stirrups and concrete contributions to shear decreased with increasing displacement ductility. The concrete contributions to the shear of the 11 tested columns conducted at NTU and 79 tested columns in the database are calculated as the summation of concrete contribution in the truss model V_{ct} and concrete arch contribution V_a. The ratio of measured to calculated $V_{ct}+V_a$ (equal to the value subtracting the shear strength provided by transverse reinforcement from the total shear strength) is plotted against the measured displacement ductility at shear failure in Fig. 13. The trend of the plotted data (best fit line in Fig. 13) suggests that the ratio of measured to calculated $V_{ct}+V_a$ decreases with increasing displacement ductility. However, Fig. 13 indicates that the shear strength provided by concrete is mildly sensitive to the displacement ductility. A parameter k_μ is proposed to take account of the influence of displacement ductility on the shear strength. The proposed k_μ, is equal to 0.7 for displacement ductility less than 3.0, and 0.7 for displacement ductility more than 7.0, with linear interpolation for displacement

Journal of Structural Engineering. Submitted November 8, 2011; accepted July 20, 2012;
posted ahead of print August 11, 2012. doi:10.1061/(ASCE)ST.1943-541X.0000677

ductility ranging from 3.0 to 7.0, as shown in Fig. 13.

Hence, the proposed shear strength of RC column can be expressed as:

$$V_n = V_s + k_\mu \left(V_{ct} + V_a \right) = k_\mu \left(1 + \frac{K_a}{K_t} \right) V_{ct} + \left(1 + \frac{k_\mu K_a}{K_t} \right) V_s \tag{21}$$

Evaluation of Proposed Model

Experimental Verification Using Test Results at NTU

Table 2 tabulates the ratio of measured to calculated shear strength for the proposed model and models from ACI 318-08 (2008), Priestley *et al*. (1994), Sezen (2002), and Ichinose (1992). The mean ratio of measured to calculated shear strength and its coefficient of variation are 1.14 and 0.09, 1.40 and 0.14, 0.83 and 0.10, 1.04 and 0.10, and 1.41 and 0.15 for the proposed model, for ACI 318-08, Priestley *et al.*, Sezen, and Ichinose, respectively. The results show that the proposed model can represent the shear strength reasonably, although it slightly underestimates the shear strength. Sezen's model has the best precision; however, for some columns the ratio of the measured to predicted strength is around 0.90, which means that this method may be unsafe for practical uses. As can be seen from Table 2, the predicted shear strength by ACI 318-08 model is relatively conservative for the SC-1.7 and RC-1.7 series of specimens, of which the shear span-to-depth ratios are small. Because the influence of axial load isn't considered in the Ichinose's model, the ratio of measured to calculated shear strength increases as the axial compression increases.

Evaluation of Proposed Model with 90 RC Columns

A compiled experimental database of 90 RC columns is utilized to evaluate the proposed model and the popular models from ACI 318-08, Priestley *et al*. (1994), Sezen (2002), and Ichinose (1992). The database consists of 11 columns carried out at NTU and 79 columns in the aforementioned literature. Fig. 14 and Fig. 15 plot the ratio of measured shear strength, V_e to calculated shear

Journal of Structural Engineering. Submitted November 8, 2011; accepted July 20, 2012;
posted ahead of print August 11, 2012. doi:10.1061/(ASCE)ST.1943-541X.0000677

strength $V_{proposed}$, V_{ACI}, $V_{Priestley\ et\ al.}$, V_{Sezen}, and $V_{Ichinose.}$ versus shear span-to-depth ratio and axial-load ratio, respectively. The correlation between the measured and calculated shear strength across the range of shear span-to-depth ratios and axial-load ratios suggests that the proposed model can predict the shear strength reasonably.

The mean ratio of measured to calculated shear strength and its coefficient of variation are 1.09 and 0.15, 1.23 and 0.27, 0.81 and 0.21, 1.13 and 0.17, and 1.08 and 0.31 for the proposed model, ACI 318-08, Priestley *et al.*, Sezen, and Ichinose, respectively. The proposed model slightly underestimates the shear strength of the RC column. There are two major reasons that account for the underestimation. Firstly, in the proposed truss-arch mode, the effective depth of the arch is derived by subtracting the thickness of concrete cover from the neutral axis depth of the section; however, in some tested columns, the concrete cover did not spall at shear failure, therefore, the arch action was underestimated. Secondly, the proposed k_{μ} in Eq. (21) is a little less than the statistical value; however, it is safe for use. From the results of comparison, there is a risk of overestimating the shear strength using Priestley *et al.*'s model, which has been approved by Sezen (2002). Using the ACI 318-08 method, the predicted shear strengths of the database are generally conservative; however, the estimate is overly conservative for small a/d and increasingly non-conservative at larger a/d. This discrepancy is caused by the effects that the arch action in the column weakens with an increase of a/d. Although the mean ratio of measured to calculated shear strength for Ichinose's model is 1.08, the coefficient of variation is relative large. As mentioned above, the ratio of measured to calculated shear strength increases as the axial compression increases, because the influence of axial load isn't considered in the Ichinose's model. Sezen's model can also predict the shear strength relatively accurately; however, for the columns with a/d

Journal of Structural Engineering. Submitted November 8, 2011; accepted July 20, 2012;
posted ahead of print August 11, 2012. doi:10.1061/(ASCE)ST.1943-541X.0000677

≤2, the predicted shear strength is comparatively conservative.

Conclusions

Observed results of 11 RC columns conducted at NTU and the collected experimental data of 79 RC columns indicate that the shear strength is significantly influenced by the shear span-to-depth ratio and axial-load ratio as the shear strength of RC column is transferred partly by the truss mechanism and partly by arch action. Considering the condition of deformation compatibility between the truss model and the arch model, a predictive expression for shear strength of shear-critical RC columns subjected to cyclic load is presented. The proposed model considers the contributions of concrete and transverse reinforcements to the shear in the truss model, as well as the shear strength provided by the arch action.

From the comparison of measured and predicted shear strengths of 90 shear-critical RC columns, the shear strength predicted by the proposed model is found to correlate well with experimental results, and the mean ratio of measured to calculated shear strength and its coefficient of variation are 1.09 and 0.15, respectively. Furthermore, the good correlation between the experimental and predicted strengths across the range of shear span-to-depth ratios and axial-load ratios indicates that the proposed method represents the effects of the two key parameters very well. The shear strengths predicted by the ACI 318-08 method are relatively conservative, especially for columns of small shear span-to-depth ratios. Comparative results also show that the model by Priestley *et al.* tends to overestimate the shear strength.

Acknowledgments

The experiments by Tran (2010) were carried out in the Protective Engineering Laboratory at the Nanyang Technological University, Singapore.

Journal of Structural Engineering. Submitted November 8, 2011; accepted July 20, 2012;
posted ahead of print August 11, 2012. doi:10.1061/(ASCE)ST.1943-541X.0000677

References

American Concrete Institute (ACI). (2008). "Building code requirements for structural concrete and commentary." *ACI Committee 318*, Farmington Hills, Mich.

Architectural Institute of Japan (AIJ). (1994). "AIJ structural design guidelines for reinforced concrete buildings." Tokyo, Japan. 207pages.

ASCE-ACI Committee 445. (1998). "Recent approaches on shear design of structural concrete." *Journal of Structural Engineering, ASCE*, 124(12), 1375-417.

Bentz, E. C., Vecchio, F. J., and Collins, M. P. (2006). "Simplified modified compression field theory for calculating the shear strength of reinforced concrete elements." *ACI Structural Journal*, 103(4), 614-624.

Bett, B. J., Klingner, R. E., and Jirsa, J. O. (1985). "Behavior of strengthened and repaired reinforced concrete columns under cyclic deformations." *PMFSEL Report No. 85-3*, Department of Civil Engineering, University of Texas at Austin.

Canadian Standards Association (CSA). (2004). "Design of concrete structures (CSA A23.3-04)." *CSA Committee*, Mississauga.

Elwood, K. J., and Moehle, J. P. (2005). "Axial capacity model for shear-damaged columns." *ACI Structural Journal*, 102(4), 578-587.

Ichinose, T. (1992). "A shear design equation for ductile RC members." *Earthquake Engineering and Structural Dynamics*, 21(3), 197-214.

Ikeda, A. (1968). *Rep.*, Training Institute for Engineering Teachers, Yokohama National Univ., Japan, also in Masaya, H. (1973). *A list of past experimental results of reinforced concrete columns*, Building Research Inst., Ministry of Construction, Japan.

Journal of Structural Engineering. Submitted November 8, 2011; accepted July 20, 2012;
posted ahead of print August 11, 2012. doi:10.1061/(ASCE)ST.1943-541X.0000677

Kim, D. J., Kim, W., and White, R. N. (1998). "Prediction of reinforcement tension produced by arch action in RC beams." *Journal of Structural Engineering, ASCE*, 124(6), 611-622.

Kim, J. H., and Mander, J. B. (1999). "Truss modeling of reinforced concrete shear-flexure behavior." *MCEER-99-0005*, Multidisciplinary Center for Earthquake Engineering Research, Buffalo, N.Y.

Kim, J. H., and Mander, J. B. (2007). "Influence of transverse reinforcement on elastic shear stiffness of cracked concrete elements." *Engineer Structures*, 29(8), 1798-1807.

Kokusho, S. (1964). *Rep.*, Building Research Inst., Tsukuba, Japan, also in Masaya, H. (1973). *A list of past experimental results of reinforced concrete columns*, Building Research Inst., Ministry of Construction, Japan.

Kokusho, S., and Fukuhara, M. (1965). *Rep.*, Kokusho Lab., Tokyo Industrial Univ., also in Masaya, H. (1973). *A list of past experimental results of reinforced concrete columns*, Building Research Inst., Ministry of Construction, Japan.

Konwinski, C., Ramirez, J.A., and Sozen, M. A. (1996). "Shear strength of reinforced concrete columns subjected to seismic loading." *Proceedings of the National Seismic Conference on Bridges and Highways: Progress in Research and Practice*, San Diego, California.

Leonhardt, F. (1965). "Reducing the shear reinforcement in reinforced concrete beams and slabs." *Magazine of Concrete Research*, 17(53), 187-198.

Lynn, A. C. (2001). "Seismic evaluation of existing reinforced concrete building columns." PhD thesis, University of California at Berkeley, Berkeley, California.

Nakamura, T., and Yoshimura, M. (2002). "Gravity load collapse of reinforced concrete columns with brittle failure modes." *Journal of Asian Architecture and Building Engineering*, 1(1),

Journal of Structural Engineering. Submitted November 8, 2011; accepted July 20, 2012;
posted ahead of print August 11, 2012. doi:10.1061/(ASCE)ST.1943-541X.0000677

21-27.

Ousalem, H. (2006). "Experimental and analytical study on axial load collapse assessment and retrofit of reinforced concrete columns." Ph.D. Thesis, University of Tokyo, Tokyo.

Paulay, T., and Priestley, M. J. N. (1992). "Seismic design of reinforced concrete masonry buildings." John Willey & Sons, N.Y.

Priestley, M. J. N., Verma, R., and Xiao, Y. (1994). "Seismic shear strength of reinforced concrete columns." *Journal of Structural Engineering, ASCE*, 120(8), 2310-2329.

Ramirez, H., and Jirsa, J. O. (1980). "Effect of axial load on shear behavior of short RC columns under cyclic lateral deformations." *PMFSEL Report* No. 80-1, University of Texas at Austin.

Saatcioglu, M., and Ozcebe, G. (1989). "Response of reinforced concrete columns to simulated seismic loading." *ACI Structural Journal*, 86(1), 3-12.

Sezen, H. (2002). "Seismic behavior and modeling of reinforced concrete building columns." PhD thesis, University of California at Berkeley, Berkeley, California.

Sezen, H., and Moehle J. P. (2004). "Shear strength model for lightly reinforced concrete columns. " *Journal of Structural Engineering, ASCE*, 130(11), 1692-1703.

Tran, C. T. N. (2010). "Experimental and analytical studies on the seismic behavior of reinforced concrete columns with light transverse reinforcement." PhD thesis, Nanyang Technological University, Singapore.

Umemura, H., and Endo, T. (1970). *Rep.*, Umemura Laboratory, Tokyo University, also in Masaya, H. (1973). "*A list of past experimental results of reinforced concrete columns*." Building Research Inst., Ministry of Construction, Japan.

Umehara, H., and Jirsa, J. O. (1982). "Shear strength and deterioration of short reinforced concrete

Journal of Structural Engineering. Submitted November 8, 2011; accepted July 20, 2012;
posted ahead of print August 11, 2012. doi:10.1061/(ASCE)ST.1943-541X.0000677

columns under cyclic deformations." *PMFSEL Report* No. 82-3, University of Texas at Austin.

Vecchio, F. J., and Collins, M. P. (1986). "The modified compression field theory for reinforced concrete elements subjected to shear." *ACI Journal Proceedings*, 83(2), 219-231.

Wight, J.K., and Sozen, M.A. (1973). "Shear strength decay in reinforced concrete columns subjected to large deflection reversals." *Structural Research Series No. 403*, Civil Engineering Studies, University of Illinois, Urbana-Champaign.

Xiao, Y., and Martirossyan, A. (1998). "Seismic performance of high-strength concrete columns." *Journal of Structural Engineering, ASCE*, 124(3), 241-251.

Yalcin, C. (1997). "Seismic evaluation and retrofit of existing reinforced concrete bridge columns." PhD thesis, Univ. of Ottawa, Ottawa.

Yoshimura, M., and Nakamura, T. (2003*a*). "Axial collapse of reinforced concrete short columns." *The 4th US-Japan Workshop on Performance-Based Earthquake Engineering Methodology for Reinforced Concrete Building Structures*, Toba, Japan, 187-198.

Yoshimura, M., Takaine, Y., and Nakamura, T. (2003*b*). "Collapse drift of reinforced concrete columns." *The 5th US-Japan Workshop on Performance-Based Earthquake Engineering Methodology for Reinforced Concrete Building Structures*, Hakone, Japan, 239-253.

Journal of Structural Engineering. Submitted November 8, 2011; accepted July 20, 2012;
posted ahead of print August 11, 2012. doi:10.1061/(ASCE)ST.1943-541X.0000677

Notations

The following symbols are used in this paper:

a = shear span, $a=L/2$ for columns with fixed-fixed ends, $a=L$ for fixed-pinned ends;

A_g = gross area of section;

A_s = main longitudinal tensile reinforcement under flexure;

A_{sv} = cross section area of transverse reinforcement at spacing s;

b = width of column;

c = thickness of concrete cover;

c_a = effective depth of strut in arch model;

d = effective depth of column;

d_v = effective shear depth taken as flexural lever arm which need not be taken less than $0.9d$;

E_c = modulus of elasticity of concrete;

E_s = modulus of elasticity of reinforcing steels;

f_c' = cylinder strength of concrete;

f_y = yielding stress of longitudinal reinforcing steels;

f_{vy} = yielding stress of transverse reinforcing steels;

h = height of column;

K_a = shear stiffness of truss model;

K_t = shear stiffness of arch model;

k_μ = factor relating concrete contributions to shear strength in truss model and concrete in arch model to displacement ductility;

L = column height;

n = E_s/E_c;

P = applied axial load on column;

s = spacing of transverse reinforcement;

s_{ze} = effective crack spacing;

V_a = shear strength provided by arch action;

V_{ct} = contribution of concrete to shear in truss model;

Journal of Structural Engineering. Submitted November 8, 2011; accepted July 20, 2012;
posted ahead of print August 11, 2012. doi:10.1061/(ASCE)ST.1943-541X.0000677

V_e = measured shear strength of column;

V_m = shear strength not considering influence of displacement ductility;

V_n = shear strength considering influence of displacement ductility;

V_s = contribution of transverse reinforcement to shear;

x = neutral axis depth;

α = inclination of strut arch;

β = factor accounting for the concrete contribution to shear in truss model;

ε_x = longitudinal strain at mid-depth of cross section;

ζ_1 = boundary condition factor of column for calculating ε_x, ζ_1 =2 for fixed-fixed ends, ζ_1 =1 for fixed-pinned ends;

ζ_2 = boundary condition factor of column for calculating θ, ζ_2=0.57 for fixed-fixed ends, ζ_2=1.57 for fixed-pinned ends;

θ = angle of the inclined strut in cracked concrete with respect to longitudinal axis of column in truss model;

μ_s= displacement ductility of RC column at shear failure;

ρ_{sl} = volumetric ratio of longitudinal reinforcement to concrete;

ρ_v = volumetric ratio of transverse reinforcement to concrete, $\rho_v = A_{sv}/(bs)$;

Journal of Structural Engineering. Submitted November 8, 2011; accepted July 20, 2012;
posted ahead of print August 11, 2012. doi:10.1061/(ASCE)ST.1943-541X.0000677

Captions to Figures

Fig. 1. Damaged columns during earthquake

Fig. 2. Truss-arch model proposed by Ichinose

Fig. 3. Model column details (Unit: mm)

Fig. 4. Backbone curves of SC-2.4 series of specimens

Fig. 5. Backbone curves of SC-1.7 series of specimens

Fig. 6. Backbone curves of RC-1.7 series of specimens

Fig. 7. Normalized shear strength versus shear span-to-depth ratio

Fig. 8. Normalized shear strength versus axial-load ratio

Fig. 9. Cracks patterns at shear failure and at axial failure

Fig. 10. Postulated diagonal cracks pattern and critical section for column with double curvatures

Fig. 11. Arch model

Fig. 12. Shear deformation of truss model

Fig. 13. Ratio of measured to calculated shear strength provided by concrete vs. displacement ductility

Fig. 14. Variation of measured to calculated strength ratio versus shear span-to-depth ratio

Fig. 15. Variation of measured to calculated strength ratio versus axial-load ratio

Journal of Structural Engineering. Submitted November 8, 2011; accepted July 20, 2012;
posted ahead of print August 11, 2012. doi:10.1061/(ASCE)ST.1943-541X.0000677

Captions to Tables

Table 1. RC Column Experimental Parameters

Table 2. Comparisons of Shear Strength between Proposed Model and Other Models

Appendix Dimensions, Materials, and Other Details for 79 Shear-Critical Columns

Journal of Structural Engineering. Submitted November 8, 2011; accepted July 20, 2012;
posted ahead of print August 11, 2012. doi:10.1061/(ASCE)ST.1943-541X.0000677

Table 1. RC Column Experimental Parameters

Specimen	f_c' (MPa)	b (mm)	h (mm)	L (mm)	$\frac{a}{d}$	$\frac{P}{f_c' A_g}$	Longitudinal steel			Transverse steel			V_e (kN)
							d_b (mm)	Num	f_{yl} (MPa)	A_{sv} (mm)	s (mm)	f_{yv} (MPa)	
SC-2.4-0.20	22.6	350	350	1700	2.7	0.20	20	8	408.0	56.5	125	392.6	218.9
SC-2.4-0.30	49.3	350	350	1700	2.7	0.30	25	8	409.0	56.5	125	392.6	357.1
SC-2.4-0.50	24.2	350	350	1700	2.7	0.50	20	8	408.0	56.5	125	392.6	237.6
SC-1.7-0.05	29.8	350	350	1200	1.9	0.05	20	8	408.0	56.5	125	392.6	276.4
SC-1.7-0.20	27.5	350	350	1200	1.9	0.20	20	8	408.0	56.5	125	392.6	294.2
SC-1.7-0.35	25.5	350	350	1200	1.9	0.35	20	8	408.0	56.5	125	392.6	335.5
SC-1.7-0.50	26.4	350	350	1200	1.9	0.50	20	8	408.0	56.5	125	392.6	375.6
RC-1.7-0.05	32.5	250	490	1700	1.9	0.05	20	8	408.0	56.5	125	392.6	283.1
RC-1.7-0.20	24.5	250	490	1700	1.9	0.20	20	8	408.0	56.5	125	392.6	305.5
RC-1.7-0.35	27.1	250	490	1700	1.9	0.35	20	8	408.0	56.5	125	392.6	345.7
RC-1.7-0.50	26.8	250	490	1700	1.9	0.50	20	8	408.0	56.5	125	392.6	355.2

Table 2. Comparisons of Shear Strength between Proposed Model and Other Models

Specimen	a/d	$P/(f_c' A_g)$	$\mu_{shear\text{-}failure}$	$V_e/V_{proposed}$	V_e/V_{ACI}	$V_e/V_{Priestley\ et\ al.}$	V_e/V_{Sezen}	$V_e/V_{Ichinose}$
SC-2.4-0.20	2.7	0.20	1.57	1.15	1.28	0.75	1.08	1.32
SC-2.4-0.30	2.7	0.30	2.38	1.07	1.11	0.78	1.06	1.60
SC-2.4-0.50	2.7	0.50	2.05	0.95	1.06	0.71	0.87	1.39
SC-1.7-0.05	1.9	0.05	1.44	1.29	1.66	0.99	1.24	1.25
SC-1.7-0.20	1.9	0.20	1.66	1.15	1.55	0.83	1.04	1.38
SC-1.7-0.35	1.9	0.35	1.14	1.15	1.61	0.87	1.05	1.64
SC-1.7-0.50	1.9	0.50	1.41	1.08	1.57	0.93	1.02	1.80
RC-1.7-0.05	1.9	0.05	1.61	1.27	1.41	0.85	1.11	1.05
RC-1.7-0.20	1.9	0.20	1.60	1.25	1.47	0.82	1.05	1.27
RC-1.7-0.35	1.9	0.35	1.63	1.13	1.40	0.79	0.97	1.38
RC-1.7-0.50	1.9	0.50	2.11	0.99	1.30	0.80	0.90	1.42
Mean				1.14	1.40	0.83	1.04	1.41
Coefficient of Variation				0.09	0.14	0.10	0.10	0.15

Journal of Structural Engineering. Submitted November 8, 2011; accepted July 20, 2012;
posted ahead of print August 11, 2012. doi:10.1061/(ASCE)ST.1943-541X.0000677

Appendix

Dimensions, Materials, and Other Details for 79 Shear-Critical Columns

Specimen	Reference	Configu-ration	f_c' (MPa)	b (mm)	h (mm)	L (mm)	ρ_s (%)	f_y (MPa)	ρ_v (%)	f_{vy} (MPa)	P (kN)	μ_s	V_e (kN)
3CLH18	Lynn (2001)	FF	25.6	457	457	2946	2.35	335	0.07	400	503	1.60	271.5
2CLH18		FF	33.1	457	457	2946	1.46	335	0.07	400	503	5.08	240.3
3SLH18		FF	25.6	457	457	2946	2.35	335	0.07	400	503	1.94	267
2SLH18		FF	33.1	457	457	2946	1.46	335	0.07	400	503	4.70	231.4
2CMH18		FF	25.7	457	457	2946	1.46	335	0.07	400	1512	1.85	316
3CMH18		FF	27.6	457	457	2946	2.35	335	0.07	400	1512	1.34	338.2
3CMD12		FF	27.6	457	457	2946	2.35	335	0.18	400	1512	2.33	356
3SMD12		FF	25.6	457	457	2946	2.35	335	0.18	400	1512	2.02	378.3
2CLD12	Sezen (2002)	FF	21	457	457	2946	1.86	469	0.18	469	667	2.21	303
2CHD12		FF	21	457	457	2946	1.86	469	0.18	469	2669	2.72	301
2CLD12M		FF	22	457	457	2946	1.86	469	0.18	469	667	4.18	295
CUS	Umehara and Jirsa (1982)	FF	34.9	230	410	910	2.40	441	0.28	414	534	1.13	324
CUW		FF	34.9	410	230	910	3.00	441	0.15	414	534	1.94	265
2CUS		FF	42	230	410	910	2.40	441	0.55	414	1068	1.06	412
No. 1-1	Bett *et al*. (1985)	FF	29.9	305	305	914	1.83	462	0.09	414	288	1.41	214
HC4-8L16-T6-0.1P	Xiao and Martirossyan (1998)	FF	86	254	254	1016	1.84	510	0.74	449	534	5.00	268
HC4-8L16-T6-0.2P		FF	86	254	254	1016	1.84	510	0.74	449	1068	3.50	324
C1	Ousalem (2006)	FF	13.5	300	300	900	1.18	340	0.08	587	364.5	3.66	160.4
C4		FF	13.5	300	300	900	1.18	340	0.28	384	364.5	4.54	171.1
C6		FF	13.5	300	300	900	1.18	340	0.28	384	243	6.42	203.9
C8		FF	18	300	300	900	1.18	340	0.28	384	486	3.90	233
C10		FF	18	300	300	900	1.18	340	0.28	384	243	4.54	262.1
C12		FF	18	300	300	900	1.18	340	0.28	384	324	4.94	217.1
D1		FF	27.7	300	300	600	1.18	447	0.43	398	540	3.27	341.1
D16		FF	26.1	300	300	600	1.18	447	0.43	398	540	3.51	341.6
D11		FF	28.15	300	300	900	1.47	447	0.14	398	540	4.25	242.8
D12		FF	28.15	300	300	900	1.47	447	0.14	398	540	4.00	250.4
D13		FF	26.1	300	300	900	1.47	447	0.43	398	540	4.33	266.1
D14		FF	26.1	300	300	900	1.47	447	0.43	398	540	4.63	296.1

Journal of Structural Engineering. Submitted November 8, 2011; accepted July 20, 2012;
posted ahead of print August 11, 2012. doi:10.1061/(ASCE)ST.1943-541X.0000677

N18M	Nakamura and Yoshimura (2002)	FF	26.5	300	300	900	1.79	380	0.19	375	429	3.03	263
N18C		FF	26.5	300	300	900	1.79	380	0.19	375	429	4.06	264
N27M		FF	26.5	300	300	900	1.79	380	0.19	375	645	4.62	288
N27C		FF	26.5	300	300	900	1.79	380	0.19	375	645	2.38	263
2M	Yoshimura and Nakamura (2003*a*)	FF	25.2	300	300	600	1.79	396	0.19	392	430	4.97	234
2C		FF	25.2	300	300	600	1.79	396	0.19	392	430	6.23	222
3M		FF	25.2	300	300	600	1.79	396	0.19	392	657	5.41	248
3C		FF	25.2	300	300	600	1.79	396	0.19	392	657	5.75	264
2M13		FF	25.2	300	300	600	1.18	350	0.19	392	430	3.07	250
2C13		FF	25.2	300	300	600	1.18	350	0.19	392	430	4.77	260
No.1	Yoshimura *et al*. (2003*b*)	FF	30.7	300	300	1200	1.79	402	0.19	392	552	2.62	234
No.3		FF	30.7	300	300	1200	1.79	402	0.09	392	552	2.55	230
No.4		FF	30.7	300	300	1200	1.79	402	0.19	392	828	2.55	261
00-U	Ramirez and Jirsa (1980)	FF	34.5	305	305	915	1.84	410	0.32	455	0	2.60	265.9
120C-U		FF	30.7	305	305	915	1.84	411	0.32	455	534	2.73	297.9
40.033*a*(E)	Wight and Sozen (1973)	FP	34.7	152	305	876	2.44	496	0.32	345	189	2.96	94
40.033*a*(W)		FP	34.7	152	305	876	2.44	496	0.32	345	189	3.05	98
40.048(E)		FP	26.1	152	305	876	2.44	496	0.46	345	178	3.93	101
40.048(W)		FP	26.1	152	305	876	2.44	496	0.46	345	178	4.35	95
40.033(E)		FP	33.6	152	305	876	2.44	496	0.32	345	178	2.71	91
40.033(W)		FP	33.6	152	305	876	2.44	496	0.32	345	178	2.87	101
25.033(E)		FP	33.6	152	305	876	2.44	496	0.32	345	111	2.49	85
25.033(W)		FP	33.6	152	305	876	2.44	496	0.32	345	111	2.32	91
40.067(E)		FP	33.4	152	305	876	2.44	496	0.64	345	178	4.88	86
40.067(W)		FP	33.4	152	305	876	2.44	496	0.64	345	178	4.57	92
40.092(E)		FP	33.5	152	305	876	2.44	496	0.91	317	178	5.36	108
40.092(W)		FP	33.5	152	305	876	2.44	496	0.91	317	178	4.83	113
U1	Saatcioglu and Ozcebe (1989)	FP	43.57	350	350	1000	2.40	430	0.30	470	0	3.12	274.9
U2		FP	30.2	350	350	1000	2.40	453	0.30	470	600	2.87	270
BR-S1	Yalcin (1997)	FP	44.8	550	550	1485	1.95	434	0.10	425	2086	2.88	578
43	Ikeda (1968)	FP	20	200	200	500	2.00	434	0.28	558	80	4.13	73.8
44		FP	20	200	200	500	2.00	434	0.28	558	80	2.56	76.5
45		FP	20	200	200	500	2.00	434	0.28	558	155.7	1.74	82.3
46		FP	20	200	200	500	2.00	434	0.28	558	155.7	1.26	80.5
62		FP	20	200	200	500	2.00	345	0.28	475.7	80	5.96	57.8
63		FP	20	200	200	500	2.00	345	0.28	475.7	155.7	4.00	68.5

Journal of Structural Engineering. Submitted November 8, 2011; accepted July 20, 2012;
posted ahead of print August 11, 2012. doi:10.1061/(ASCE)ST.1943-541X.0000677

64		FP	20	200	200	500	2.00	345	0.28	475.7	155.7	4.82	68.5
205	Umemura and Endo (1970)	FP	17.58	200	200	600	2.00	462	0.28	324	155.7	2.51	71.2
207		FP	17.58	200	200	400	2.00	462	0.28	324	155.7	1.60	105.9
208		FP	17.58	200	200	400	2.00	462	0.28	324	391	2.99	135.2
214		FP	17.58	200	200	600	2.00	462	0.14	324	391	1.73	82.7
220		FP	32.9	200	200	400	1.00	379	0.11	648	155.7	7.83	78.3
231		FP	14.75	200	200	400	1.00	324	0.13	524	155.7	8.42	50.7
232		FP	13.1	200	200	400	1.00	324	0.13	524	155.7	6.40	58.3
233		FP	13.9	200	200	400	1.00	372	0.13	524	155.7	4.50	68.9
234		FP	13.1	200	200	400	1.00	372	0.13	524	155.7	5.33	67.2
372	Kokusho (1964)	FP	20	200	200	500	1.00	524	0.31	351.6	241	4.12	74.3
373		FP	20.4	200	200	500	2.00	524	0.31	351.6	241	2.78	88.1
452	Kokusho and Fukuhara(1965)	FP	21.9	200	200	500	3.00	358	0.31	606	391	2.53	110.3
454		FP	21.9	200	200	500	4.00	358	0.31	606	391	2.32	110.3

Noted: “FF” in “Configuration” Column means tested columns with fixed-fixed ends which is the confinement of the test column, and “FP” means columns with fixed-pinned ends.

Journal of Structural Engineering. Submitted November 8, 2011; accepted July 20, 2012;
posted ahead of print August 11, 2012. doi:10.1061/(ASCE)ST.1943-541X.0000677

(*a*) 2009 Padang Earthquake, Indonesia (*b*) 2011 Christchurch Earthquake, New Zealand

Fig. 1. Damaged columns during earthquake

Journal of Structural Engineering. Submitted November 8, 2011; accepted July 20, 2012;
posted ahead of print August 11, 2012. doi:10.1061/(ASCE)ST.1943-541X.0000677

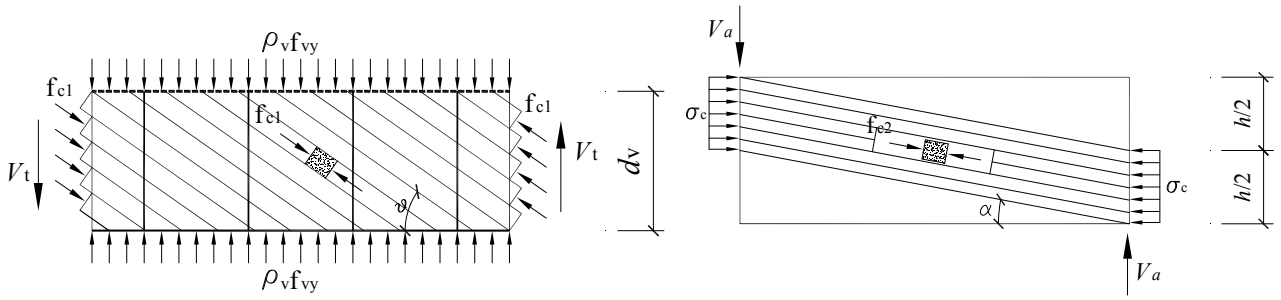

(*a*) Truss model (*b*) Arch model

Fig. 2. Truss-arch model proposed by Ichinose

Journal of Structural Engineering. Submitted November 8, 2011; accepted July 20, 2012;
posted ahead of print August 11, 2012. doi:10.1061/(ASCE)ST.1943-541X.0000677

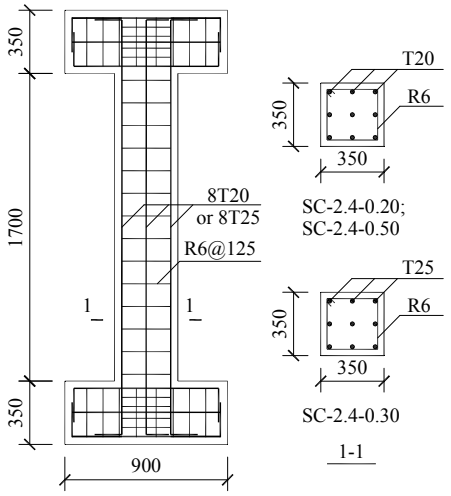

(*a*) SC-2.4 series of specimens

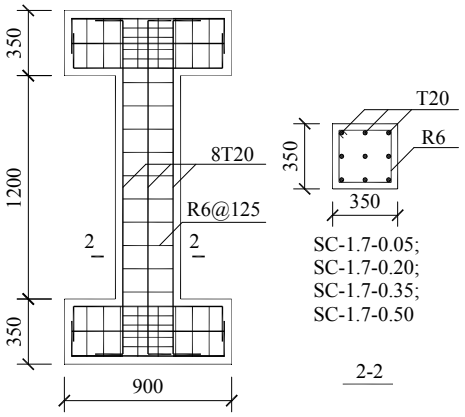

(*b*) SC-1.7 series of specimens

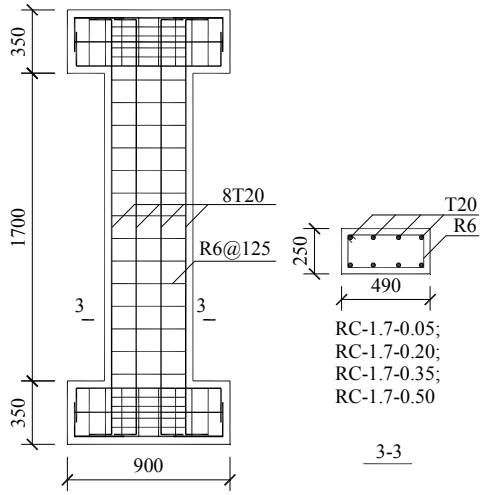

(*c*) RC-1.7 series of specimens

Fig. 3. Model column details (Unit: mm)

Journal of Structural Engineering. Submitted November 8, 2011; accepted July 20, 2012;
posted ahead of print August 11, 2012. doi:10.1061/(ASCE)ST.1943-541X.0000677

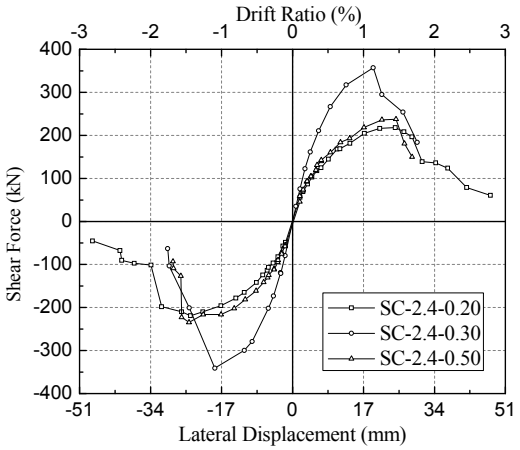

Fig. 4. Backbone curves of SC-2.4 series of specimens

Fig. 5

Journal of Structural Engineering. Submitted November 8, 2011; accepted July 20, 2012;
posted ahead of print August 11, 2012. doi:10.1061/(ASCE)ST.1943-541X.0000677

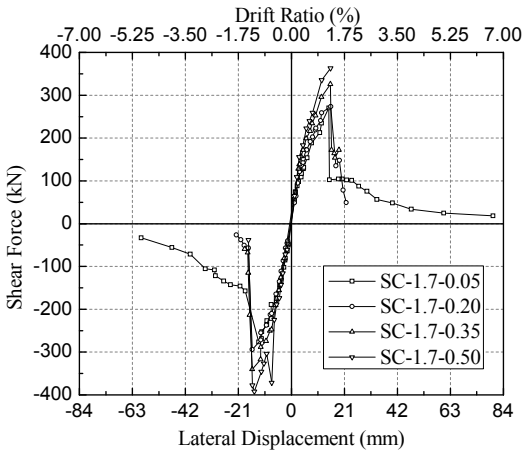

Fig. 5. Backbone curves of SC-1.7 series of specimens

Fig. 6

Journal of Structural Engineering. Submitted November 8, 2011; accepted July 20, 2012;
posted ahead of print August 11, 2012. doi:10.1061/(ASCE)ST.1943-541X.0000677

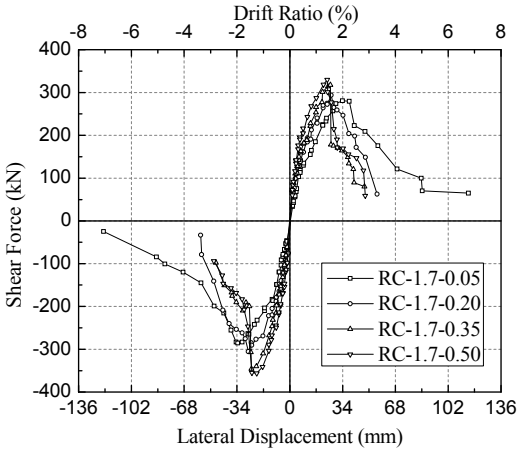

Fig. 6. Backbone curves of RC-1.7 series of specimens

Journal of Structural Engineering. Submitted November 8, 2011; accepted July 20, 2012;
posted ahead of print August 11, 2012. doi:10.1061/(ASCE)ST.1943-541X.0000677

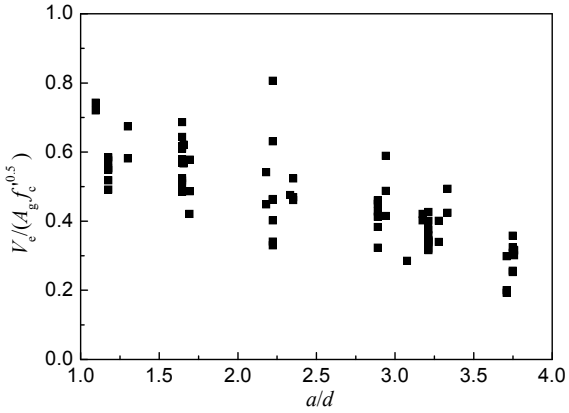

Fig. 7. Normalized shear strength versus shear span-to-depth ratio

Fig. 8

Journal of Structural Engineering. Submitted November 8, 2011; accepted July 20, 2012;
posted ahead of print August 11, 2012. doi:10.1061/(ASCE)ST.1943-541X.0000677

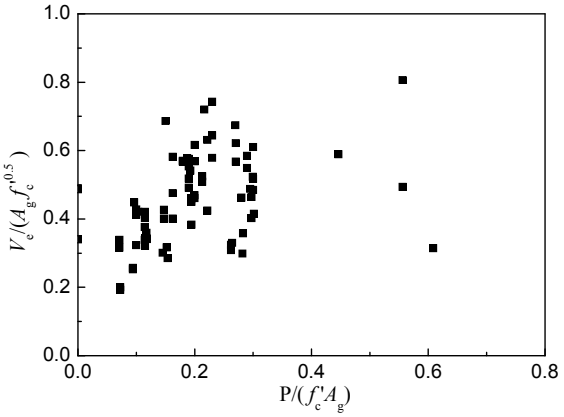

Fig. 8. Normalized shear strength versus axial-load ratio

Journal of Structural Engineering. Submitted November 8, 2011; accepted July 20, 2012;
posted ahead of print August 11, 2012. doi:10.1061/(ASCE)ST.1943-541X.0000677

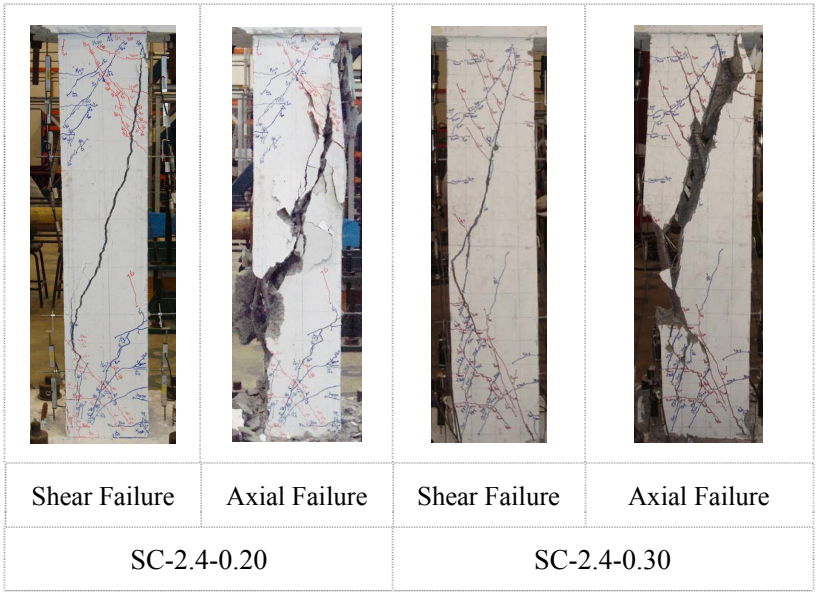

Fig. 9. Cracks patterns at shear failure and at axial failure

Fig. 10

Journal of Structural Engineering. Submitted November 8, 2011; accepted July 20, 2012;
posted ahead of print August 11, 2012. doi:10.1061/(ASCE)ST.1943-541X.0000677

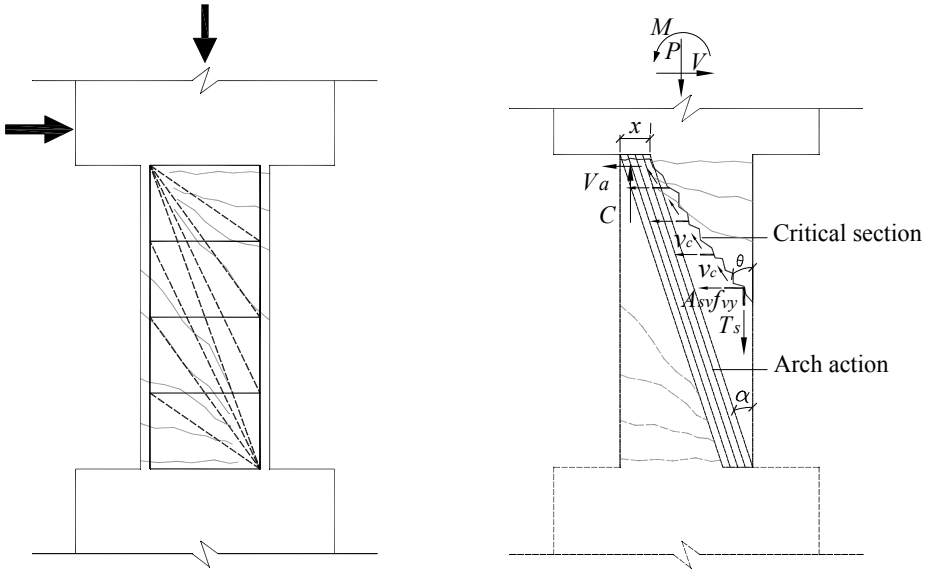

(*a*) Postulated distribution of diagonal cracks (*b*) Schematic critical section

Fig. 10. Postulated diagonal cracks pattern and critical section for column with double curvatures

Fig. 11

Journal of Structural Engineering. Submitted November 8, 2011; accepted July 20, 2012;
posted ahead of print August 11, 2012. doi:10.1061/(ASCE)ST.1943-541X.0000677

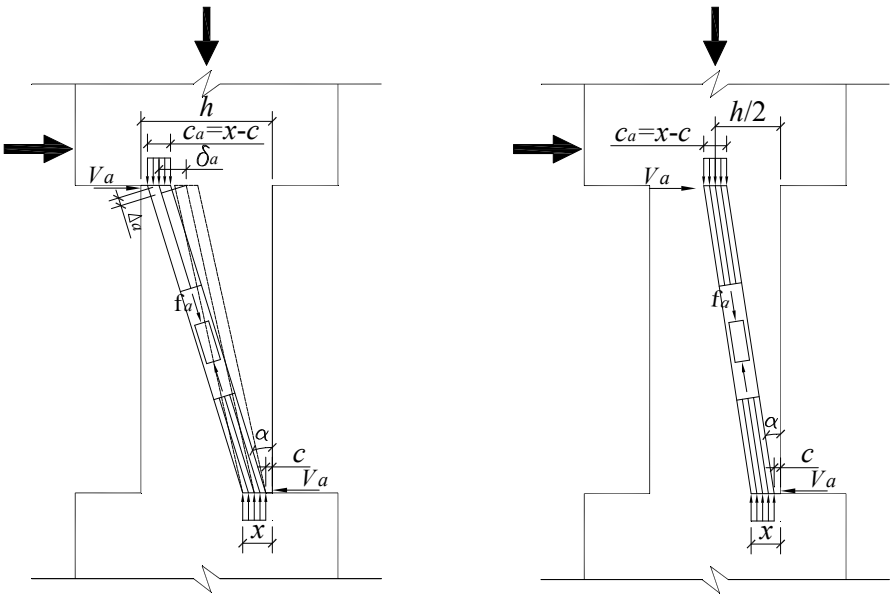

(*a*) Columns with fixed-fixed ends (*b*) Columns with fixed-pinned ends

Fig. 11. Arch model

Fig. 12

Journal of Structural Engineering. Submitted November 8, 2011; accepted July 20, 2012;
posted ahead of print August 11, 2012. doi:10.1061/(ASCE)ST.1943-541X.0000677

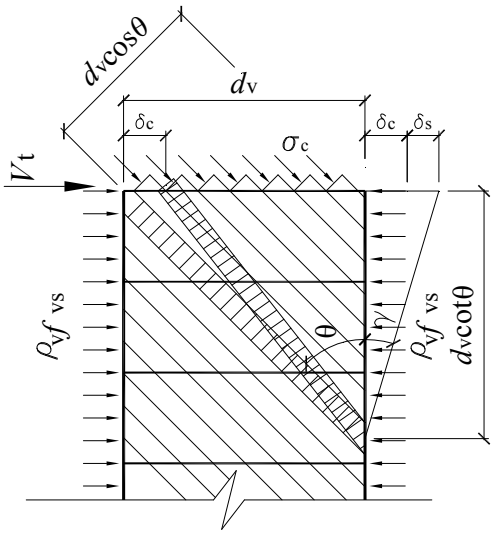

Fig. 12. Shear deformation of truss model

Journal of Structural Engineering. Submitted November 8, 2011; accepted July 20, 2012;
posted ahead of print August 11, 2012. doi:10.1061/(ASCE)ST.1943-541X.0000677

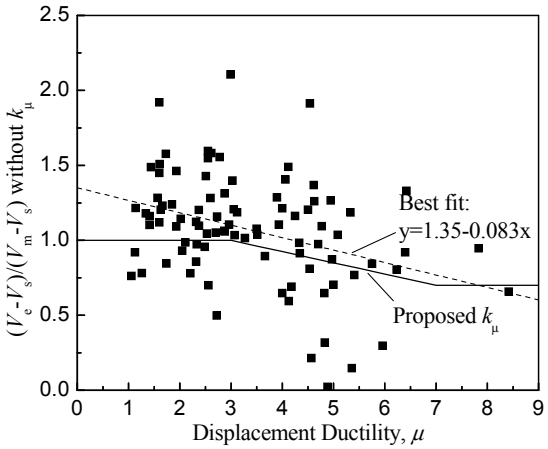

Fig. 13. Ratio of measured to calculated shear strength provided by concrete vs. displacement ductility

Journal of Structural Engineering. Submitted November 8, 2011; accepted July 20, 2012;
posted ahead of print August 11, 2012. doi:10.1061/(ASCE)ST.1943-541X.0000677

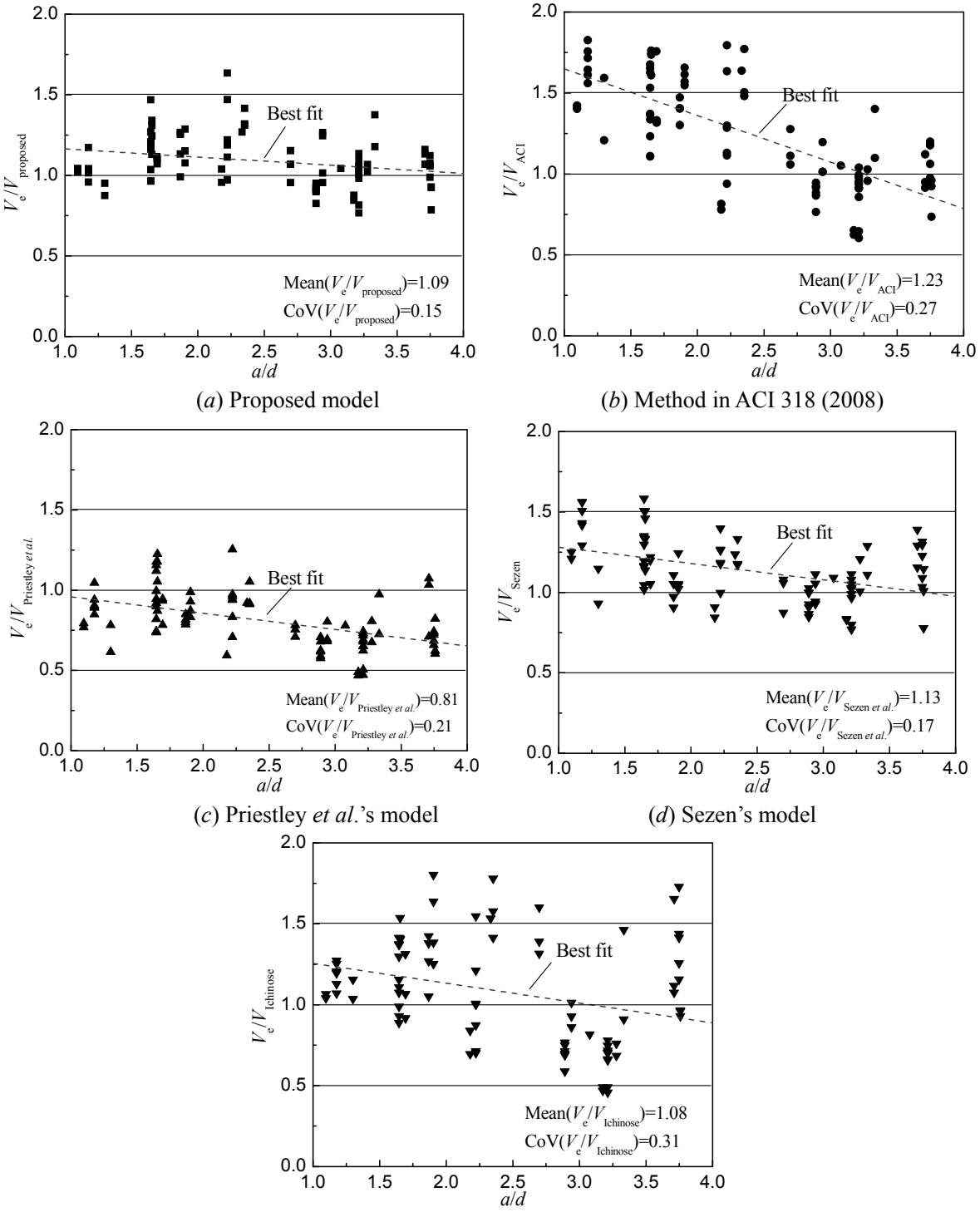

Fig. 14. Variation of measured to calculated strength ratio versus shear span-to-depth ratio

Journal of Structural Engineering. Submitted November 8, 2011; accepted July 20, 2012;
posted ahead of print August 11, 2012. doi:10.1061/(ASCE)ST.1943-541X.0000677

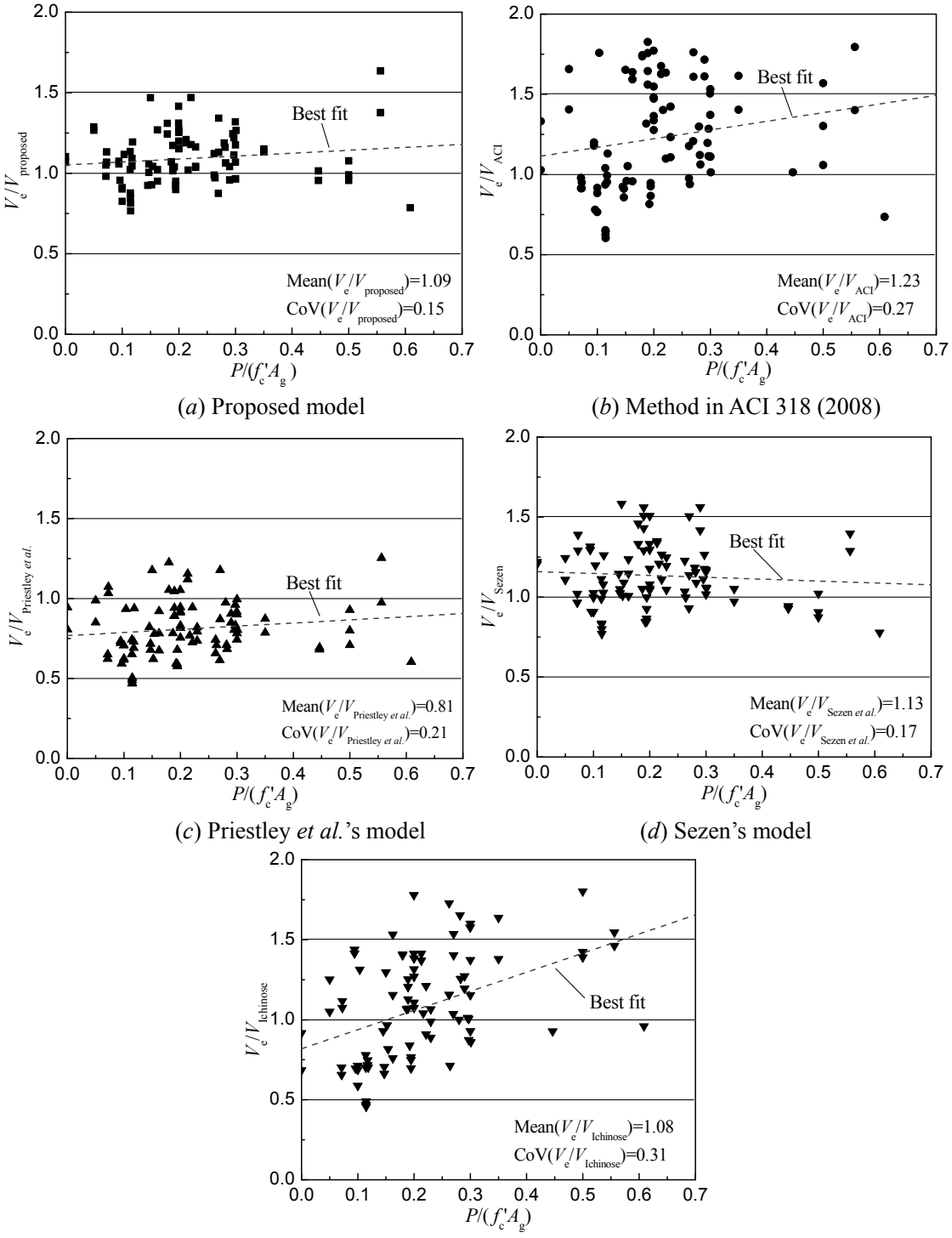

(*a*) Proposed model (*b*) Method in ACI 318 (2008)

(*c*) Priestley *et al.*'s model (*d*) Sezen's model

(*e*) Ichinose's model

Fig. 15. Variation of measured to calculated strength ratio versus axial-load ratio